SCIENTIFIC JOURNAL
EARTH'S CRYOSPHERE

Earth's Cryosphere, 2016, vol. XX, No. 1, pp. 34–45 **http://earthcryosphere.ru/**

CRYOGENIC PROCESSES AND FORMATIONS

MULTISTAGE HOLOCENE MASSIVE GROUND ICE IN NORTHERN WEST SIBERIA

Yu.K. Vasil'chuk, N.A. Budantseva, A.C. Vasil'chuk, Ye.Ye. Podborny*, Ju.N. Chizhova

Lomonosov Moscow State University, Geography and Geology Departments,
1, Leninskie Gory, Moscow, 119991, Russia; vasilch_geo@mail.ru
**Hydroecological Research Center, 16A, Nalichnaya str., St. Petersburg, 199406, Russia; epodbornyy@yandex.ru*

Four lenses of massive ground ice and three cryopegs have been discovered at different levels in Holocene deposits in the northeastern Yamal Peninsula near Sabetta Village. Lateral and vertical $\delta^{18}O$ isotope patterns in multistage massive ice from the Sabetta and Gyda estuaries evidence of its heterogeneity and intrasedimental origin by segregation or by a combined intrusive-segregation mechanism. Cl^-/SO_4^{2-} ratios, spore-pollen spectra, and the presence of algae in the Sabettayakha massive ice have implications for the origin of its different types. Columnar brown ice formed by freezing of sand saturated with water of the Ob Gulf, monolith brown ice is a frozen lake talik, while ultra-fresh white ice originates from lake and stream waters. Massive ground ice occurs in pre-Quaternary consolidated deposits, as well as in Holocene and modern sediments.

Holocene, massive ice, permafrost, cryopegs, Yamal Peninsula, northern West Siberia

INTRODUCTION

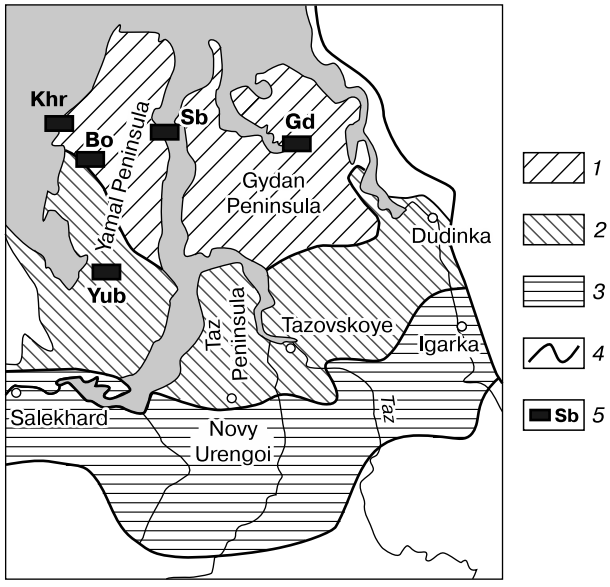

Fig. 1. Location map of massive ground ice occurrences in northern West Siberia.

1, *2* – permafrost, almost continuous from the surface (northern zone): low-temperature genetically heterogeneous (syngenetic over epigenetic) permafrost in tundra (*1*) and higher-temperature mainly epigenetic permafrost in forested tundra (*2*); *3* – discontinuous permafrost (northern taiga); *4* – boundaries of permafrost zones and subzones; *5* – massive ice occurrences: Sb – layda and Sabettayakha terrace I; Bo – Seyakha floodplain in the Bovanenkovo gas-condensate field; Khr – terrace I near Kharasavei Village; Yub – Yuribei floodplain (Yamal); Gd – Gyda terrace I.

Massive ground ice in permafrost is a complex periglacial phenomenon, and its origin is still poorly understood. This is a separate macro-scale geocryological element which brings much engineering-geological complexity and poses problems to design, construction, and maintenance of structures. Most of hazard is expected from massive ice in shallow permafrost and Holocene deposits in areas under active industrial development.

In this study, we compare the structure and composition of massive ground ice bodies within the Holocene first lagoon-marine terrace and the modern laida in northern West Siberia (Fig. 1) with their possible equivalents in other Holocene occurences.

MULTISTAGE MASSIVE GROUND ICE IN THE YAMAL-GYDAN PROVINCE

At the time being, massive ground ice has been well documented in Holocene sediments of the Sabettayakha mouth and the floodplain of the Seyakha (Mutnaya) River in Yamal.

Multistage massive ground ice in the Sabettayakha mouth was found in boreholes within the low first terrace and laida (vegetated saline coastal mud flat) of the Ob Gulf (Fig. 2). Data on several drill sections from the area discussed in our previous publication [*Vasil'chuk et al., 2015*] are now extended with reports from new transects.

Massive ice in laida most often occurs within sands, except for a single body lying over a thin silt

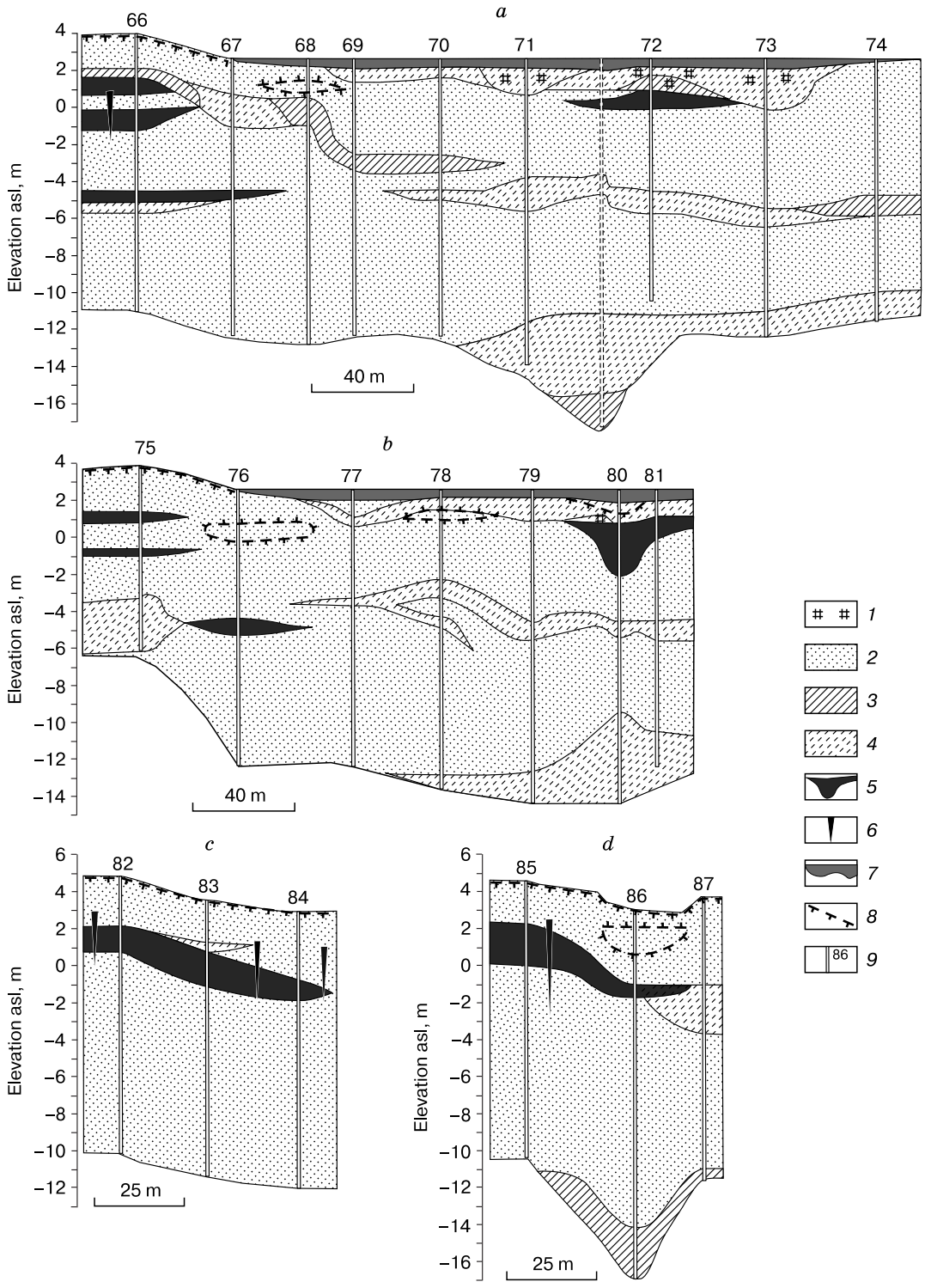

Fig. 2. Massive ground ice in Holocene laida (*a*, *b*) and terrace I (*c*, *d*), Ob Gulf near Sabetta, northeast Yamal.

1 – peat; *2* – sand; *3* – clay silt; *4* – silt; *5* – massive ice; *6* – wedge ice; *7* – surface ice; *8* – boundary between frozen and unfrozen sediments; *9* – borehole and its number.

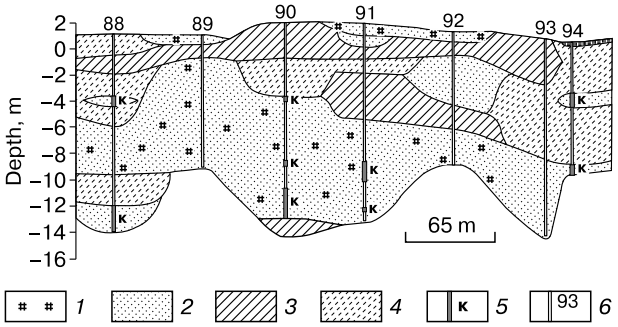

Fig. 3. Cryopegs in Holocene laida, Ob Gulf near Sabetta Village.

1 – peat; *2* – sand; *3* – clay silt; *4* – silt; *5* – cryopegs; *6* – borehole and its number.

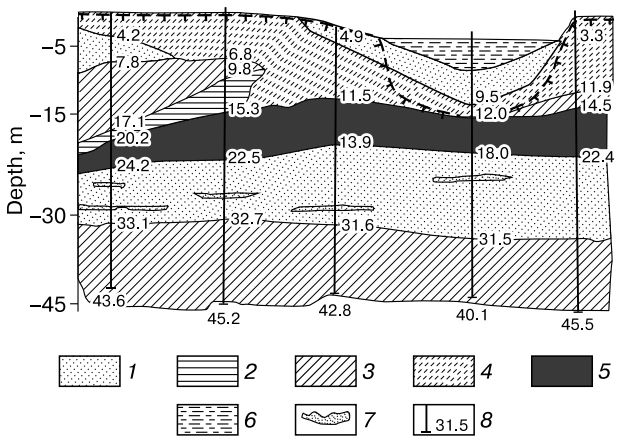

Fig. 4. Holocene massive ice under the Seyakha River and within the floodplain (according to data collected by *TyumenNIIgiprogaz* Company) [*Vasil'chuk, 2012*].

1 – sand; *2* – clay; *3* – clay silt, *4* – silt; *5* – massive ice; *6* – stream water; *7* – lenses of silty sand; *8* – borehole and depth levels.

layer (Fig. 2, *a*, BH 66) and varies in thickness and depth. Three lenses of massive ice, about 1 m or slightly thinner, were found at three levels (2, 4 and 8 m below the surface) in several boreholes: 66, 67 (Fig. 2, *a*), 75, and 76 (Fig. 2, *b*); the deepest lens may be longer than 50 m (Fig. 2, *a*). About 3 m thick ice was revealed in BH 80 (Fig. 2, *b*) at the depth 2–5 m.

Massive ice in terrace I forms lenses and layers, 2 m or thicker and over 50 m long (Fig. 2, *c*, *d*), extending into the laida. Some shallow bodies enclose wedge ice.

Multistage *cryopegs* occur at three levels (4–5 m, 8–9 m, and 11–13 m) in fourteen boreholes drilled in saline Holocene peaty sands of the Sabettayakha mouth (Fig. 3). The cryopegs appear to have originated independently, even though lie at the same depths. Several cryopegs differ in pressure head and salinity and thus have no hydraulic connection. The cryopegs have chloride-magnesian or chloride-sodium compositions and a salinity of 62.35–93.10 g/L. The ice temperatures vary from –5.2 to –5.6 °C.

Massive ice in the Seyakha floodplain is from 7 to 9 m thick (Fig. 4) and most likely represents a single body. It lies 12 m below the surface under the Seyakha River and deeper on both sides of the floodplain: at 20 m on one side and 1.0–1.5 m shallower on the other side. The ice is sandwiched between fine sand below and silt, clay silt, and clay above. The base of a closed talik under the Seyakha reaches the ice top.

Massive ice in Gyda River terrace I near Gyda village coexists with syngenetic wedge ice (Fig. 5). Ice layers in peaty sand are 0.4 m thick and 8 m long. The terrace was deposited in pre-Holocene time, 10–14 Kyr BP [*Vasil'chuk, 2011*], but its section is critical for understanding the origin of multistage massive ground ice and for interpretation of stable isotope patterns.

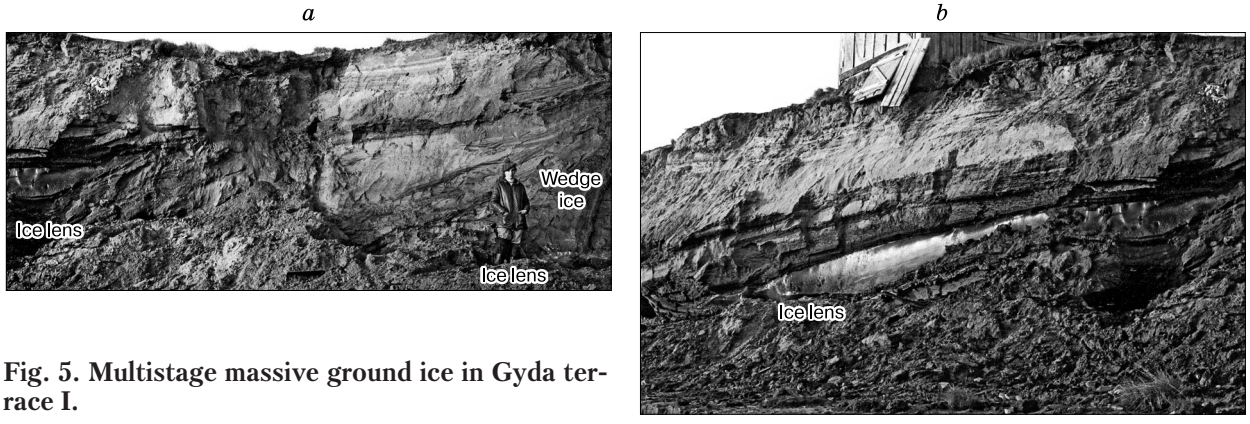

Fig. 5. Multistage massive ground ice in Gyda terrace I.

a – general view: two ice lenses, the lower one cut by syngenetic wedge ice; *b* – enlarged middle ice lens. Photograph by Yu. Vasil'chuk.

Major ions, pollen spectra, and stable isotope ratios in massive ground ice

Major ions. The salinity of the studied ice samples varies from 10.92 to 229.28 mg/L with prevalence of chlorides.

Ultra-fresh columnar brown ice in sand has a salinity of 40.64 mg/L, a major-ion composition of Cl^-, SO_4^{2-}, and Mg^{2+}, and pH = 7.9. It contains 29.14 equivalent % of carbonates, possibly, because of gradual freezing *in situ*. The Cl^-/SO_4^{2-} ratio in the ice (0.96) is similar to that in the Ob Gulf water (0.84) (Table 1, Fig. 6) [*Fotiev, 1999*]. Its slightly higher sulfate enrichment reasonably results from freezing of saturated sand [*Korenovskaya and Tarasov, 1968*].

The ultra-fresh monolith brown ice has a salinity of 81.9 mg/L, mainly Cl^-, Na^+ ion composition, pH = 6.7–7.5, and Cl^-/SO_4^{2-} = 9.77. The anion ratio, as well as the contents of cations and anions, are similar to the average values for fresh massive ice in Yamal [*Fotiev, 1999*], and for the Kara Sea water. Another sample of this ice shows high salinity of 229.28 mg/L, a Cl^-, Na^+ ion composition, neutral pH, and a Cl^-/SO_4^{2-} ratio as high as 68.91. Note that the contents of SO_4^{2-} are often low in cryopegs, especially under river channels. This sample of monolith brown ice has direct analogs among fresh and brackish ground ice samples we found elsewhere. Similar values of Cl^-/SO_4^{2-} are observed in river taliks of the Ob basin (27.67) and in average compositions of the Yamal brackish massive ice (26.39) [*Fotiev, 1999*]. Organic micro-inclusions in brown monolith ice were dated on 17 December 2015 at the Radiocarbon Laboratory of Oxford University to be 5932 ± 39 yr BP (OxA-X-2650-57).

White ice is the freshest of all Sabettayakha samples: its salinity is 10.92–13.52 mg/L; although being ultra-fresh, it has a Cl^-, Mg^{2+} and Cl^-, Ca^{2+} ion composition, and pH = 8.00–8.01; the Cl^-/SO_4^{2-} ratio is in the range 3.29–4.95. Similar chemical composition was reported for layered ice [*Fotiev, 1999*] and stream waters in Yamal, with Cl^-/SO_4^{2-} of 4.30 and 4.67, respectively, for the ice and for the streams of the Kara Sea basin.

The major ion chemistry of the Sabettayakha massive ground ice varieties records recharge from groundwaters, as well as from lacustrine, palustrine, and meteoric waters. Their composition has implications for the origin: columnar brown ice formed by freezing of sand saturated with water of the Ob Gulf, monolith brown ice is a frozen lake talik, while ultra-fresh white ice originates from lake and stream waters.

Pollen spectra. Spore and pollen concentrations in the Sabettayakha massive ice vary from almost

Table 1. **Chloride and sulfate ions in massive ice and its possible water sources (northern West Siberia)**

Object	Concentration, mg/L		Cl^-/SO_4^{2-}	Reference
	Cl^-	SO_4^{2-}		
Brown ice, BH 12, sample 8	70.61	7.23	9.77	[*Vasil'chuk et al., 2015*]
Brown ice, BH 12, sample 9	75.80	1.10	68.91	
White ice, BH 17, sample 38	55.67	11.25	4.95	
White ice, BH 17, sample 39	55.61	16.92	3.29	
Columnar brown ice, BH 42, sample 40	34.53	35.92	0.96	
Segregated ice, terrace I, Belyy Island	14.2	13.2	1.08	[*Vasil'chuk and Vasil'chuk, 2015*]
Massive ice, terrace III, Naduiyakha River	24	17	1.41	[*Streletskaya and Leibman, 2002*]
Atmospheric precipitation, northern Yamal	7	9	0.78	
Stream water, Seyakha River	12	10	1.20	
Snow pack, northern Yamal, Seyakha valley	7	13	0.54	
Cryopeg, Naduiyakha valley	37 778	764	49.45	
Fresh massive ice (average), Yamal	62.4	6.2	10.06	[*Fotiev, 1999*]
Sea water, Kara Sea	89.0	10.0	8.9	
Brackish massive ice (average), Yamal	95.0	3.6	26.39	
River taliks, Ob Gulf basin	83.0	3.0	27.67	
Ultra-fresh massive ice (average), Yamal	36.9	12.6	2.93	
Snow, Yamal	45.5	6.8	6.69	
Lake water	39.8	5.3	7.51	
Segregated ice	54.2	12.6	4.30	
Stream waters, Kara Sea	64.4	13.8	4.67	
Stream waters	25.6	11.8	2.17	
Rainfall, Yamal	32.6	18.7	1.74	
Water, Ob Gulf	27.0	32.0	0.84	
Intrusive ice	31.4	20.2	1.55	

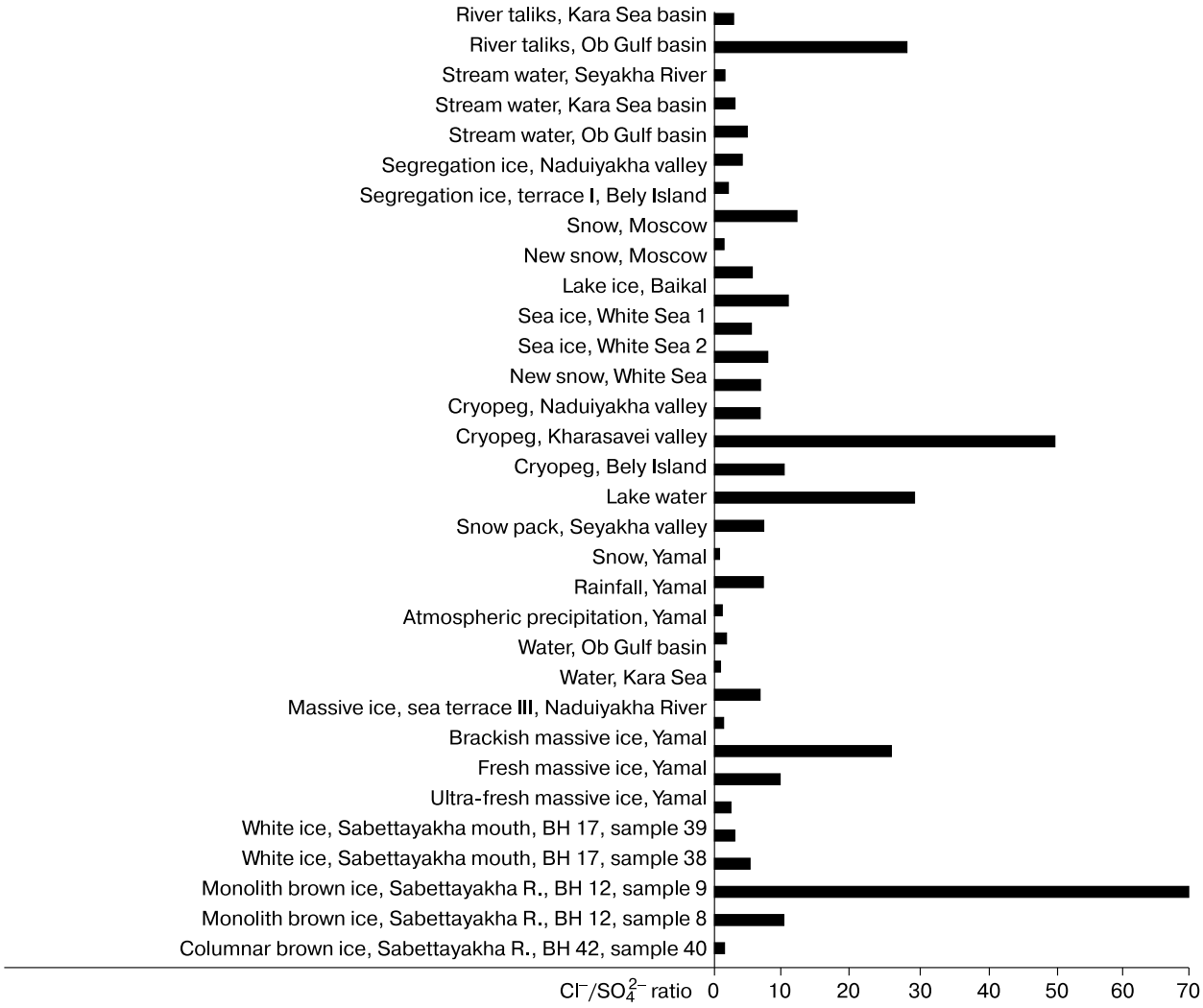

Fig. 6. Cl^-/SO_4^{2-} ratios in massive ice, waters, and snow in northern West Siberia and other cryosphere objects (measured in a single run, for better comparison).

zero in some layers to 361 grains/L, as well as remnants of *Pediastrum* algae, coal particles, and fungi spores. The concentration of spore and pollen is the greatest (361 grains/L) in sample 11 from BH 42, with a strongly depleted $\delta^{18}O$ composition (–26.04 ‰). The spore-pollen spectra of ice show its possible intrasedimental origin, while the presence of algae indicates ice formation by freezing of lake taliks or near-bottom waters of the Ob Gulf. Similar pollen spectra were obtained from multistage massive ice in the Gyda mouth [*Vasil'chuk and Vasil'chuk, 2010*].

Stable isotopes. Oxygen and deuterium isotope compositions (^{18}O and D ratios) measured in different types of the Sabettayakha Holocene massive ground ice were discussed in detail in [*Vasil'chuk et al., 2015*]. Here we only note that the samples of brown columnar ice from BH 42 show clustering rather than a linear trend in the $\delta^{18}O$–δD diagram (Fig. 7). Therefore, the ice either originated in stable intrasedimental conditions with equilibrium isotope fractionation, or is a buried homogeneous body of river ice or gulf floe. The latter idea is, however, inconsistent with strongly depleted $\delta^{18}O$ and δD (to –26.5 and –199.7 ‰, respectively). It is hard to imagine selective deposition during ice burial. If it were so, the ice-on period would have been marked by isotopic shifts at the top and base of the ice lens, while their absence supports the intrasedimental origin.

The $\delta^{18}O$ values in the Gyda massive ice are highly differentiated, with contrasts up to 4–9 ‰ within single bodies (Table 2, Fig. 8) and exceeding 18 ‰ (–34.3 against –16.2 ‰) between different lenses. In coeval wedge ice, this difference ranges from –22.5 to –19.9 ‰ ($\delta^{18}O$ in wedge ice records average $\delta^{18}O$ contents in winter precipitation). Al-

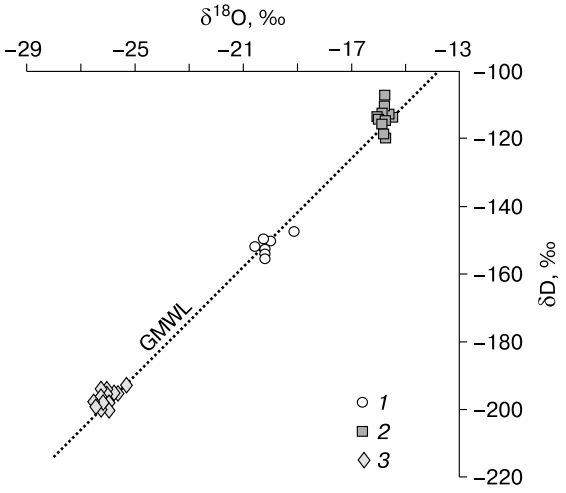

Fig. 7. δD–δ^{18}O diagram for Holocene massive ground ice near Sabetta Village.

1 – monolith brown ice, BH 12; *2* – white layered ice, BH 17; *3* – columnar brown ice, BH 42; GMWL is Craig's Global Meteoric Water Line.

Table 2. **δ^{18}O patterns in massive ice, Gyda terrace I, northern Gydan Peninsula**

Ice lenses	Depth, m	δ^{18}O, ‰
Lens 1	4.6	–30.1
	4.5	–34.3
	4.4	–30.7
Lens 2	4.15	–17.7
Lens 3	3.7	–22.9
	3.5	–24.2
	3.1	–20.1
Lens 4	2.9	–23.3
	2.8	–16.2

though being highly variable and randomly distributed, δ^{18}O values in massive ice generally increase upwards (Fig. 8, *b*). The surface and ground waters of the Gyda area appear to feed from summer rainfall as well. The δ^{18}O differentiation may be a consequence of closed-system ice-water fractionation during freezing of the source aquifer, with δ^{18}O of –20 to –18 ‰. More evidence for this hypothesis comes from unusually low δ^{18}O (less than –30 ‰) in the lowermost ice lens. Such strongly depleted δ^{18}O values are known neither from modern surface waters of the area nor from Late Pleistocene ice in the Yamal and Gyda peninsulas [*Vasil'chuk, 1992*]. They may result from fractionation during freezing, which is consistent with intrasedimental formation of ice lenses in the Gyda first terrace.

Thus, some δ^{18}O patterns among vertical and lateral variations of oxygen isotope compositions

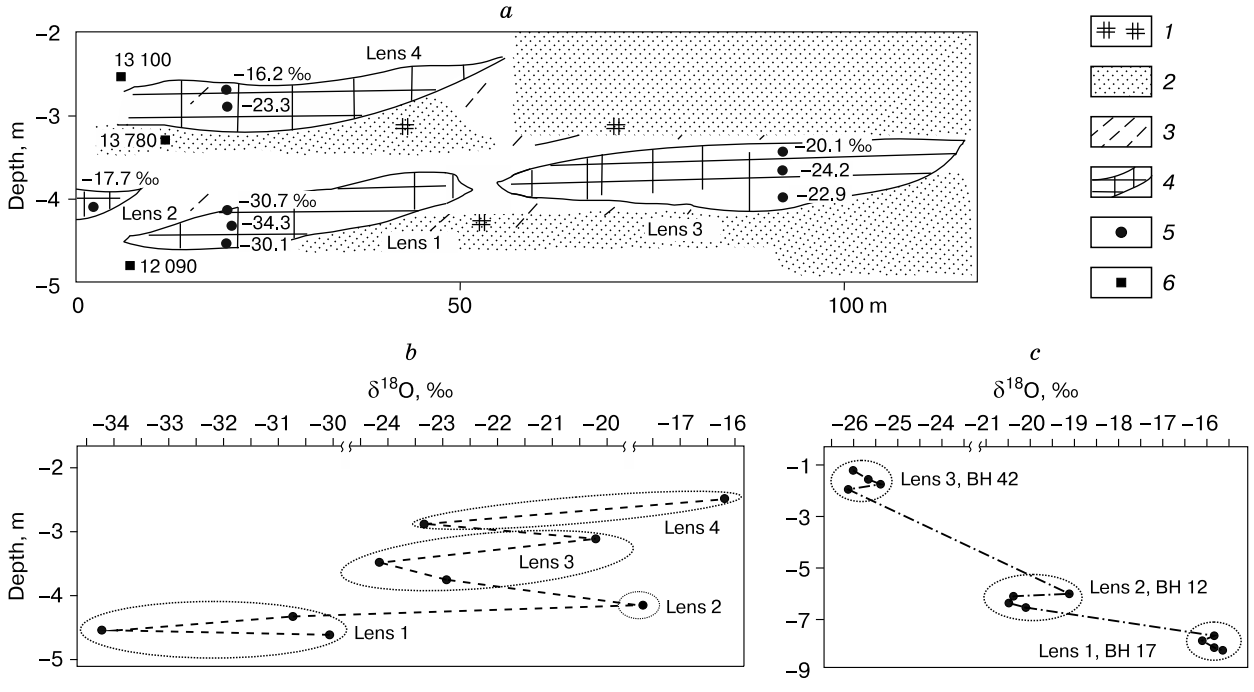

Fig. 8. δ^{18}O patterns in multistage homogeneous segregation ice and syngenetic wedge ice in Gyda terrace I (*a*) and vertical δ^{18}O variations in ice lens in Gyda mouth (*b*), compared with contrasting δ^{18}O values in three lenses of the Sabettayakha multistage massive ice in Holocene lagoon-marine terrace I and laida (*c*):

1 – allochthonous peat and dispersed detritus; *2* – sand; *3* – silt; *4* – lenses of massive ice; sites of sampling for δ^{18}O (*5*) and ^{14}C (*6*). Dash line contours isotope values in each ice lens.

(Fig. 8, *b*, *c*) can be diagnostic of segregation or intrusive-segregation origin of multistage ice; intrasedimental massive ice is marked by high variability of $\delta^{18}O$ values.

Stable isotope ratios of river and lake ice in the Liard River basin (left tributary of the Mackenzie River, northern Canada) show the following distribution: −24.4 ‰ $\delta^{18}O$, −201 ‰ δD in snow; ≈ −15 ‰ $\delta^{18}O$, ≈−130 ‰ δD in river ice (0.76 m thick); and ≈ −17.5 ‰ $\delta^{18}O$, ≈ −140 ‰ δD in water under ice at a depth of 1 m. The respective values for Goose Lake in the Liard floodplain show stronger isotope depletion, with $\delta^{18}O$ = −27.3 ‰, δD = −219 ‰, in snow; weaker depletion in snow-ice layer ($\delta^{18}O$ = −18 ‰, δD = −150 ‰); and still more enriched isotopic ratios of −15 to −14 ‰ $\delta^{18}O$ and −140 to −122 ‰ δD in ice [*Gibson and Prowse, 1999, 2002*]. Deuterium excess in the ice of two Liard tributaries (d_{exc}) varies in a large range as a result of congelation: it decreases from 0 to −6 ‰ and then increases +6 ‰ down the 87 cm thick section of river ice in one tributary and decreases from 0 to −18 ‰ in 38 cm thick ice in the other tributary [*Gibson and Prowse, 1999, 2002*]. The authors attribute the difference in the ice d_{exc} patterns between the two streams to their feeding from lake or wetland sources. The absence of notable d_{exc} vertical trend in brown columnar ice from BH 42 likewise contradicts river the ice burial hypothesis [*Vasil'chuk et al., 2015*].

Holocene massive ice in marine and lagoon bottom sediments

There are several occurrences of Holocene massive ice in marine and lagoon sediments.

Mechigmen Gulf (East Chukotka): saline massive ice, a ~1.5 m thick lens, discovered (by Yu. Vasil'chuk) while studying the drilling results from a shallow-water borehole, which encountered permafrost under more than 10 m of water.

Khatanga mouth: cryopegs (lenses of highly saline water, up to 97 g/L) and massive ice. Cryopegs were discovered (by *Ponomarev* [*1961*]) at ~10 m in a borehole drilled in the tidal zone. The cryopegs overlie clay silt with thin ice layers, soot inclusions and

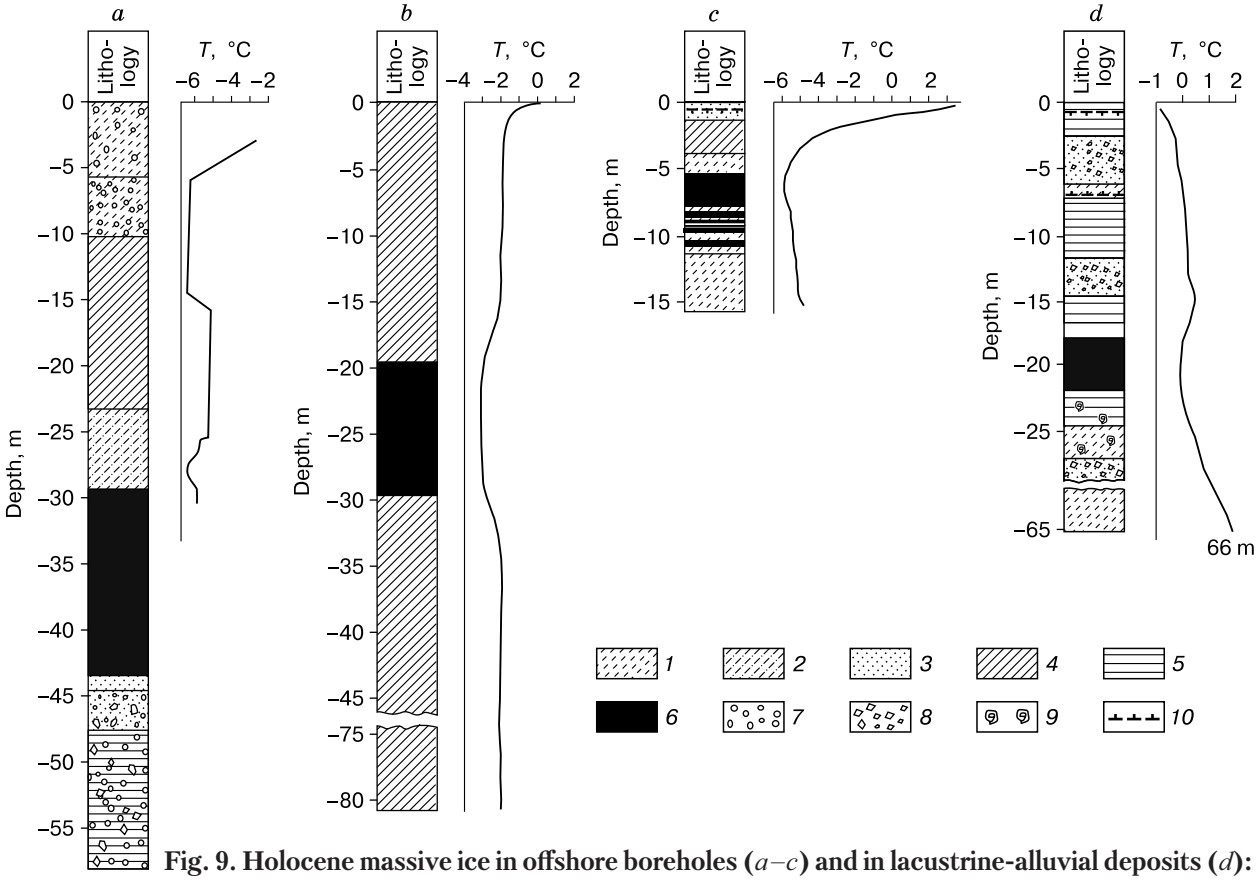

Fig. 9. Holocene massive ice in offshore boreholes (*a*–*c*) and in lacustrine-alluvial deposits (*d*):

a – borehole that revealed 14 m thick massive ice (beach zone flooded by tides, Cape Kozhevnikov, near Khatanga mouth) [*Ponomarev, 1961*]; *b* – offshore borehole BH 240 in Baidarata Bay, water depth 13 m, 12 km from Yamal Peninsula, massive ice about 10 m thick [*Melnikov and Spesivtsev, 1995*]; *c* – beach borehole BH 1 that revealed about 6 m thick massive ice, vicinity of Kharasavei Village (September 1978) [*Grigoriev, 1987*]; *d* – borehole BH 6 that revealed 4.45 m thick massive ice, northern Lake Elin, source region of Yellow River (China) [*Wang and Li, 1990*]; *1* – silt; *2* – silty clay; *3* – sand; *4* – clay silt; *5* – clay; *6* – ice; *7* – pebble; *8* – gravel and debris; *9* – spiral-shaped fossils; *10* – permafrost boundary.

peat containing pressurized (1.8 bar) methane (Fig. 9, *a*). Clay silt, in turn, lies over 13.5 m of dense ice with sand in the upper part, with its temperature from –4.5 to –5.5 °C, while the saline water temperature is –5.5 °C. According to *V.M. Ponomarev* [*1961*], the ice lens possibly melted on the margins when it became flooded, but ice degradation stopped as sand and clay over it became progressively thicker due to beach subsidence [*Ponomarev, 1961*].

Baidarata Gulf: massive ice [*Melnikov and Spesivtsev, 1995*] in a 80 m deep borehole (BH 240) drilled under 13 m of water, 12 km offshore near Yamal. The borehole tapped permafrost top at 17 m below the sea bottom (Fig. 9, *b*). Frozen sediments to the 19 m subbottom depth consist of dark grey clay silt with inherited layered cryostructure and a clay content of 70 vol.%. The 19–29 m interval includes fresh (0.62 g/L) Holocene massive ice, with mineral material (clay silt debris) between 26 and 29 m. No ice appears below 32 m. The ground temperature is ~1 °C colder within massive ice and ice-rich sediments (Fig. 9, *b*) but is 1 °C warmer above and below ice and remains invariable (–2.0, –2.2 °C) all along the section [*Melnikov and Spesivtsev, 1995*].

Beach near Kharasavei village: Holocene massive ice interlayered with silt, about 6 m thick (Fig. 9, *c*), encountered at a borehole depth of 5.5 m. Ice lies below the sea level and is colder than the host sediments [*Grigoriev, 1987*].

Holocene massive ice in young terraces, floodplains, and laida

Isotope data are available for few bodies of massive ice near Kharasavei village, on the Slider River in Arctic Canada, and in the upper stream of the Yellow River (Huang He).

North bank of Lake Elin: massive ice in the watershed areas of the Yellow River (Huang He) and Lake Hubei (elevation 4300 m asl, mean annual air temperature –4.2 °C) in China [*Wang and Li, 1990*]. Permafrost in the borehole between 3.0 and 16.5 m depth (T = –0.65 °C) is slightly saline in 16.5–18.8 and 24.26–200.8 m intervals, with a subzero temperature, and encloses a 4.45 m thick pure ice lens between 18.8 and 24.26 m (Fig. 9, *d*).

Massive ice with its temperature –0.1 °C is ultrafresh (no more than 0.02 g/L) and has mainly hydrocarbonate chemistry (over 75 %). It lies between two cryopegs: the one above has a temperature of –0.65 °C, a salinity exceeding 10 g/L, and a chemistry with more than 41 % chlorides and 22 % sulfates (unlike the sediments above); the parameters of the cryopeg below are: T = –0.15 °C; ~0.9 g/L; over 83 % of chlorides. The oxygen isotope $\delta^{18}O$ composition of ice is –11.16 to –11.70 ‰ (–77.9 to –83.2 ‰ δD), is similar to that of the Urumqi glacier firn (–11.22 ‰ $\delta^{18}O$) and is within the range for glacier ice in the southern slope of a West Kunlun glacier at the snow line (from –10.0 to –12.1 ‰ $\delta^{18}O$) [*Wang and Li, 1990*]. Proceeding from these data, we (suggested by **Yu. V.**) infer it to be most likely Holocene segregated ice, while *Wang and Li* [*1990*] interpret it as Late Pleistocene deep-buried lake ice. The segregation origin of the ice is further supported by warm negative temperatures of the host sediments which can have become positive at minor warming. The most essential argument is the oxygen isotope composition of the ice identical to that of modern firn and more enriched than in Pleistocene ice from this area of the Tibetan Plateau: cf. $\delta^{18}O$ from –10 to –11 ‰ in the Holocene ice of the Dunde glacier and below –13 ‰ in Pleistocene ice [*Thompson et al., 1989*].

***Terrace I, vicinity of Kharasavei village*:** almost 4 m thick Holocene massive ground ice [*Dubikov, 2002*]. The Holocene age is indicated by available ^{14}C dates of ~9 kyr BP [*Vasil'chuk, 1992*] and is consistent with greater isotope enrichment compared to Holocene wedge ice at the same site: –10.6 ‰ $\delta^{18}O$ and = –112 ‰ δD (Fig. 10, *a*) against (–15.9 to –14.1 ‰ $\delta^{18}O$ [*Vasil'chuk, 1992*]). Massive ice from terrace III near Kharasavei is more depleted (–13.4 to –18.4 ‰ $\delta^{18}O$ and to –141 ‰ δD) [*Dubikov, 2002; Kritsuk, 2010*]). Note that ice from terraces I and III shares similar mineral contents from 10 to 90 mg/L. According to *Belova* [*2014*], ice of terrace III has a still more depleted composition of –18.6 to –26.3 ‰ $\delta^{18}O$ (–21.9 ‰ on average) and –143.1 to –197.5 ‰ δD. Judging by its oxygen isotopic signatures, ice in terrace I formed in the Holocene [*Vasil'chuk, 2012*] from summer or mixed (summer and winter) waters, while floe burial is unlikely.

***Russkii Zavorot Cape*:** homogeneous Holocene segregated massive ice found [*Velikotsky, 2001*] in a borehole within a sand bar of the Pechora Bay rising 1–3 m above the sea level. Massive ice thicker than 1.2 m (Fig. 10, *b*) lies within a 3.2 m thick layer of sand above a zone of cryopegs, up to 7 m thick, in sand and bouldery clay silt. The ice top lies 0.6–1.1 m below the surface and is conformal to the terrain: higher elevated within topographic highs (1.8–2.4 m asl) and lower (to 0.7 m asl) beneath the lows. The ice base corresponds to the sea level [*Velikotsky, 2001*].

Yuribei floodplain, Yamal: massive ice predicted by GPR and electric tomography data about 40 km upstream of the river mouth [*Olenchenko and Shein, 2013*]. Ice appears in the resistivity pattern as a 50 000 Ohm·m layer, about 15 m thick, lying most likely below the depths 4–6 m at the confluence of the Yuribei and the Yartasyo (Fig. 10, *c*, *d*). Ice wedge filling frost cracks produces nearly vertical resistivity highs and joins massive ice in the deep. The top of massive ice subsides abruptly near the Yuribei and Yartasyo Rivers, which produce a talik by their warming effect. Note the absence of river talik under the old Yuribei channel (at 50 m of the profile) where the warming effect of water is much weaker.

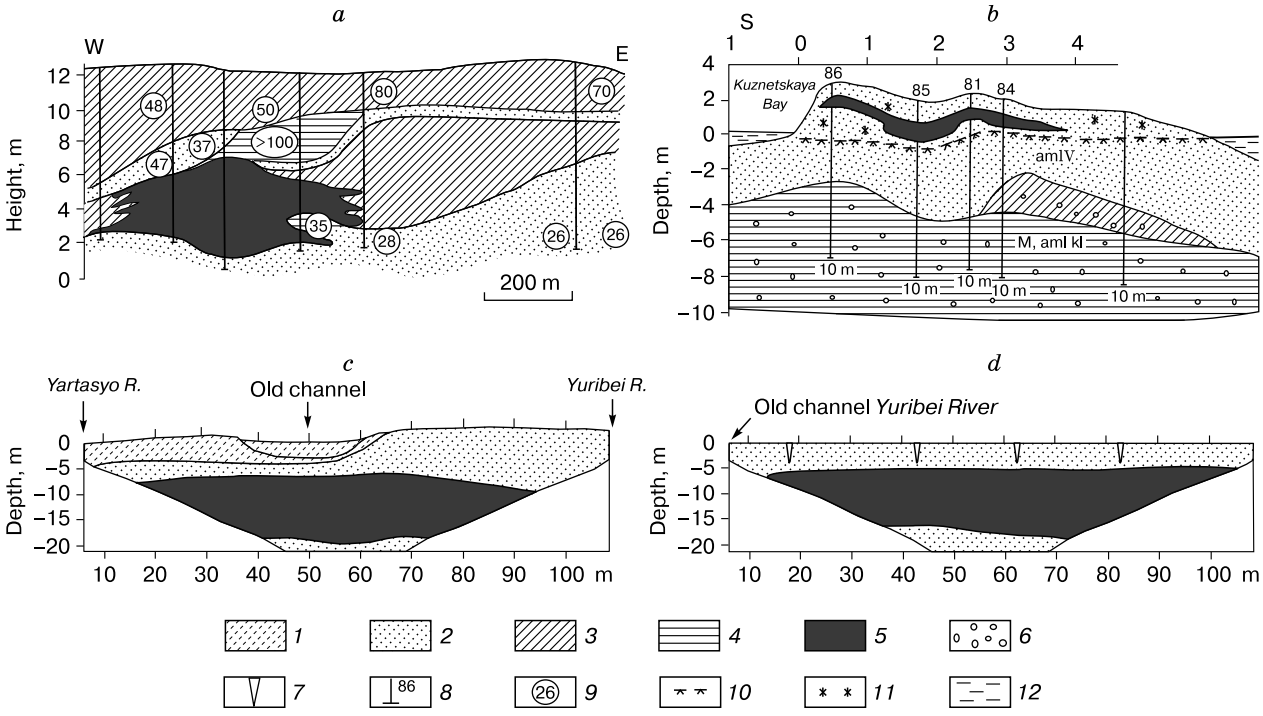

Fig. 10. Massive ice in Holocene floodplain and marine (beach) deposits.

a – massive ice, about 6 m thick, in a Holocene marine terrace near Kharasavei village [*Dubikov, 2002*]; *b* – modern segregated massive ice, over 1 m thick, in a sand bar at Cape Russkii Zavorot [*Velikotsky, 2001*]; *c*, *d* – section of the Yuribei floodplain (western Yamal), with about 15 m thick massive ice, based on resistivity data [*Olenchenko and Shein, 2013*] along profiles 1 (*c*) and 2 (*d*). *1* – silt; *2* – sand; *3* – clay silt; *4* – clay; *5* – ice; *6* – pebble; *7* – frost cracks and ice wedges; *8* – borehole and its number; *9* – water content; *10* – cryopegs; *11* – massive cryostructure in sand above cryopegs; *12* – sea water.

Two bodies of massive ice were found at 2 to 10 m and about 30 m below the surface (Fig. 11) in boreholes drilled in Late Pleistocene and Holocene deposits in a 20 km long zone of the Mordyiyakha, Seyakha, and Naduiyakha interfluve (by the R&D Institute of Engineering Geology for Construction, Tyumen) [*Streletskaya and Leibman, 2002*]. Late Pleistocene marine sand also encloses cryopegs lying

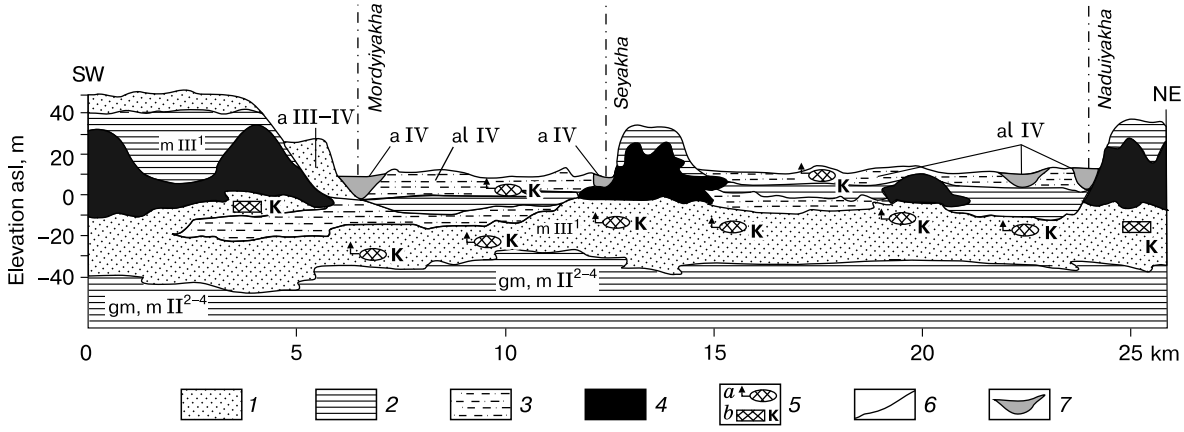

Fig. 11. Quaternary deposits with cryopegs and massive ice, Seyakha, Mordyiyakha, and Naduiyakha upper reaches, western Central Yamal [*Streletskaya and Leibman, 2002*].

1 – sand; *2* – clay; *3* – intercalated sand, clay silt, and clay; *4* – massive ice; *5* – observed (*a*) and inferred (*b*) cryopegs; *6* – boundary with the massive ice complex; *7* – rivers. gm and mII^{2-4} = Middle Pleistocene glacial-marine and marine deposits; $mIII^{1}$ = Late Pleistocene marine deposits; aIII–IV = Late Pleistocene-Holocene alluvium; aIV = Holocene alluvium; alIV = Holocene alluvial and lacustrine deposits.

about the same depth level as the lower ice body. There is another occurrence of massive ice in the floodplain at the Seyakha-Naduiyakha confluence (Fig. 11).

Fosheim Peninsula, Ellesmere Island: abundant Holocene massive ground ice as ice sills, segregated massive ice (2–3 m thick) and ice wedges (up to 7 m) [*Robinson and Pollard, 1998*] exposed in a bluff of the western bank of Hot Weather creek, 2.5 km north of its confluence with the Slider River, at 79°58′ N, 84°28′ W (Fig. 12, *a*). The mean annual air temperature in the area is 19.7 °C with a mean annual amplitude of 43 °C. Deglaciation of the area was underway by ~9.5 kyr BP [*Pollard and Bell, 1998*]. Unweathered outcrops in the Hot Weather valley consist of fining-upward poorly cemented white quartzose sandstone and coal cycles, often with interbedded mudstone and shale. Bedrock is covered by unconsolidated Holocene marine silts and fluvial silty sand [*Robinson and Pollard, 1998*].

Thick (8–9 m) Holocene segregated massive ice was studied in an outcrop on the Slider near Eureka Sound fiord [*Pollard and Bell, 1998*] (Fig. 12, *b*). The ice sandwiched between marine silts and silty clay above, with a conformable and gradational contact, and unweathered Tertiary sandstone below. The $\delta^{18}O$ values range between –28.9 to and –34.8 ‰ for reticulate ice from marine silts and silty clay, –33.0... –36.8 ‰ for massive ice, and –36.0 ‰ in a vertical ice vein in the nearby exposure of Tertiary sandstone. The $\delta^{18}O$ values of the enclosing sediments are similar to those of the massive ice. This similarity suggests a common water source, which precipitated in a very cold climate according to the isotopic signatures. The vertical $\delta^{18}O$ variations (Fig. 12, *b*) may be due to ice-water fractionation during intrasedimental ice formation.

Pollard and Bell [*1998*] interpret the Fosheim Peninsula massive ice as intrasedimental because it is conformably overlain by marine sediments and contains internal structures parallel to the upper ice contact. The presence of poorly permeable silts and silty clay above and highly permeable coarse sandstone below, which provided sufficient water supply, was favorable for ice segregation. Cracks in rocks could act as groundwater conduits in pressurized porous bedrock. Water intruded from deeper sediments under high pressure into the confining frozen ground. Both segregated and intrusive massive ice of the Eureka Sound fiord are obviously Middle Holocene, younger than 7–8 Kyr [*Pollard and Bell, 1998; Robinson and Pollard, 1998*].

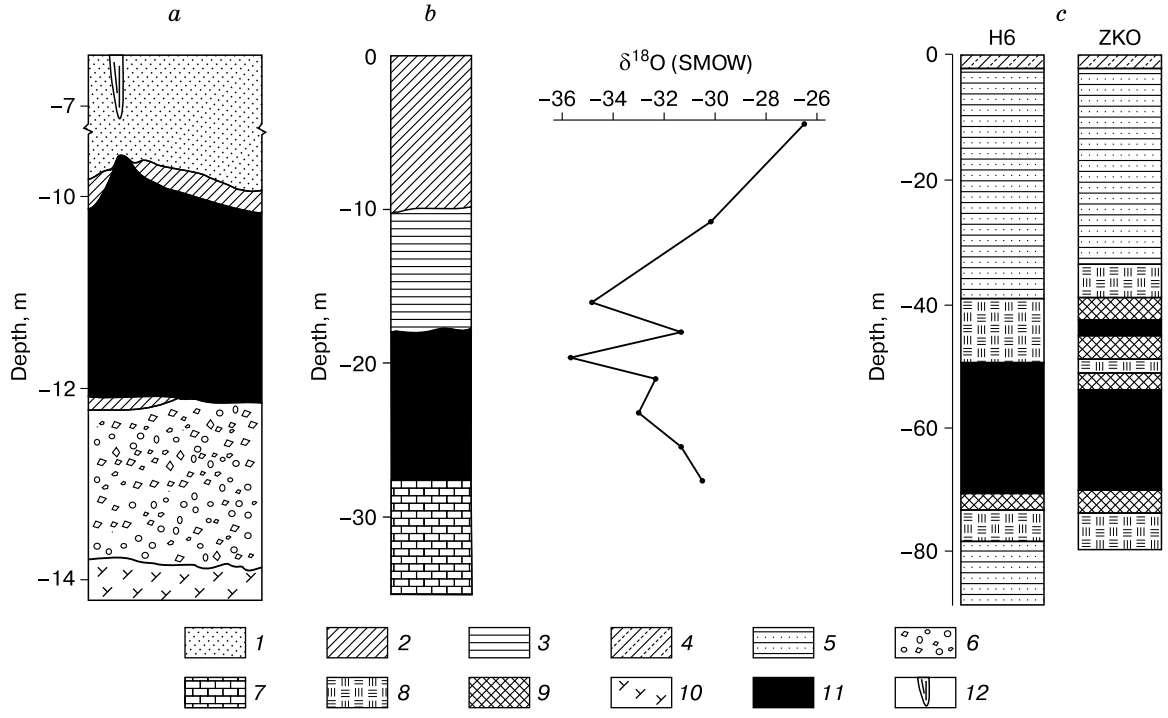

Fig. 12. Intrasedimental massive ice overlying pre-Quaternary bedrock, Fosheim Peninsula, Ellesmere Island, Canada (*a*, *b*) and enclosed in pre-Quaternary bedrock, Huola River, northeast China (*c*).

a – stratigraphic section of unit A, Hot Weather Creek, Fosheim Peninsula, Ellesmere Island [*Robinson and Pollard, 1998*]; *b* – stratigraphy and $\delta^{18}O$ variations in massive ice, up to 9 m thick, outcrop on Slider River, Eueka Sound fiord [*Pollard and Bell, 1998*]; *c* – massive ice bodies in boreholes H6 (over 20 m thick) and ZKO (1.8 and 16.45 m thick) in pre-Quaternary bedrock, Huola basin [*Wang, 1990*].

1 – sand; *2* – clay silt; *3* – clay; *4* – Quaternary deposits; *5* – sandstone; *6* – gravel and cobbles; *7* – weathered Tertiary bedrock; *8* – coal; *9* – carbonaceous mudstone; *10* – reworked Eureka Sound silt; *11* – massive ice; *12* – ice wedge.

Huola River basin, northeast China: massive ice in Jurassic conglomerates lying under 40 m of fine and coarse sandstone [*Wang, 1990*]. Borehole ZKO drilled in 1985 stripped two bodies of massive ice, 1.8 m and 16.45 m thick, in the intervals 40.0–41.8 m and 49.16–65.30 m, respectively (Fig. 12, *c*), separated by 7.35 m of coaly mudstone. Massive ice in another borehole (H6) is over 20 m thick. Ice is slightly contaminated with silt particles and has a salinity of 0.5 g/L. The ice base coincides with the base of permafrost over unfrozen mudstone. According to *Wang* [*1990*], the massive ground ice formed by *in situ* freezing of groundwater intruded under pressure and is thus intrusive ice, while we **(Yu.V.)** would rather classify it as segregated ice because unfrozen fractured mudstone hardly can have provided a screen required for intrusion of such a large amount of water.

Sibiryakov Island, Kara Sea: a lens of transparent Holocene ice, up to 1.5 m thick and 10 m long [*Opokina et al., 2010*], with a rough irregular base and a smooth sharp top. Lake ice is cut by Holocene ice wedges along which the ice base and peat layers warp up to 0.2–0.5 m. The massive ice has an enriched oxygen isotope composition with –14.4 to –17.1 ‰ $\delta^{18}O$ and –108.8 to –121.2 ‰ δD, while the wedge ice is more depleted, with –18.8 to –21.1 ‰ $\delta^{18}O$ and –141.4 to –157.9 ‰ δD [*Opokina et al., 2010; Streletskaya et al., 2012*].

The Sabettayakha (Yamal) massive ice most likely formed by freezing of sand and clay bottom sediments, as well as sand of emergent bars and isles, in a closed lagoon which lost connection with the sea. Massive ice in terrace I and laida of the Ob Gulf near Sabetta is mainly of syngenetic segregation or combined intrusive-segregation intrasedimental origin, produced by freezing of water-saturated sediments.

Some massive ice may result from catastrophic burial of shore or floating ice. Brown color may be due to ice contamination with limnic mud, because a layer of fresh black mud occurs in monolith brown ice in Sabettayakha BH 12 [*Vasil'chuk et al., 2015*]. The ice layers in Holocene sediments appear to be heterogeneous.

The bottom of the marine tidal zone and, possibly, also lagoons, lakes, and rivers, which emerged during shoaling and draining, abound in small lagoons and lakes connected by small streams and creeks [*Usov, 1967; Khimenkov, 1985*]. Freezing of such zones produces mosaic patterns as dry necks between lagoons and lakes freeze up earlier, while closed or open taliks remain beneath water bodies. Thus, there appear pockets of unfrozen saturated sediments confined by frozen sediments, which arise especially often in the case of closed taliks and shallow permafrost. The pockets shrink progressively upon further drainage as water leaves isolated lagoons and lakes. While the pockets are freezing, the expulsed pressurized water intrudes into sediments and forms intrusive-segregated ice with oblique to vertical layers.

CONCLUSIONS

1. Low lagoon-marine terraces in the northeastern Yamal Peninsula near Sabetta Village host a multistage complex of massive ground ice consisting of four lenses about 1–3 m thick and over 50 m long at the depths 1–8 m.

2. Saline sediments near Sabetta Village enclose cryopegs (salinity up to 93 g/L) at three levels.

3. Massive ice, 7 to 9 m thick, occurs at the depth 12 m under the Seyakha (Mutnaya) River.

4. Multistage massive ground ice (four lenses, 0.4 m thick and 8 m long) exists in Gyda terrace I.

5. Lateral and vertical $\delta^{18}O$ patterns in the Sabetta and Gyda multistage massive ice complexes indicate their heterogeneity and intrasedimental origin by segregation or a combined intrusive-segregation mechanism.

6. Cl^-/SO_4^{2-} ratios, spore-pollen spectra, and the presence of algae have implications for the origin of the Sabettayakha massive ice of different types. Namely, columnar brown ice formed by freezing of sand saturated with water of the Ob Gulf, monolith brown ice formed by freezing of a lake talik, while ultra-fresh white ice originated from lake and stream waters.

7. Spore-pollen spectra of the Sabettayakha massive ice are likewise consistent with its intrasedimental origin, while the presence of algae suggests freezing of lake taliks or bottom sediments of the Ob Gulf.

8. Comparison of the Sabettayakha massive ground ice in Holocene sediments with that of other permafrost sites shows that such ice is often found in obviously non-glacial deposits.

9. The presence of massive ground ice in diverse non-glacial deposits (fully or partly consolidated pre-Quaternary rocks to Holocene and modern beach, terrace, floodplain, or laida soft sediments, or below the sea bottom) means that some occurrences of Pleistocene ice likewise may be of intrasedimental origin rather than being buried glacier ice.

The paper profited much from constructive criticism by Professor V.T. Trofimov.

The study was supported by grant 14-27-00083 from the Russian Science Foundation.

References

Belova, N.G., 2014. Massive Ice in the Southwestern Kara Sea Coast. MAKS Press, Moscow, 180 pp. (in Russian)

Dubikov, G.I., 2002. Lithology and Cryostratigraphy of Sediments in West Siberia. GEOS, Moscow, 246 pp. (in Russian)

Fotiev, S.M., 1999. Formation of the ion-salt composition of natural waters in Yamal. Kriosfera Zemli III (2), 40–65.

Gibson, J., Prowse, T., 1999. Isotopic characteristics of ice cover in a large northern river basin. Hydrol. Process. 13, 2537–2548.

Gibson, J., Prowse, T., 2002. Stable isotopes in river ice: identifying primary over-winter streamflow signals and their hydrological significance. Hydrol. Process. 16, 873–890.

Grigoriev, N.F., 1987. Permafrost in the Yamal Coast. IMZ SO AN SSSR, Yakutsk, 112 pp. (in Russian)

Khimenkov, A.N., 1985. Cryostratigraphy of Marine Sediments. Author's Abstract. Candidate Thesis, Geology & Mineralogy, Moscow, 23 pp. (in Russian)

Korenovskaya, I.M., Tarasov, M.N., 1968. Major ion composition and mineralization of fresh ice formed at different conditions. Gidrokhim. Materialy XLVII, 77–87.

Kritsuk, L.N., 2010. Massive Ground Ice of West Siberia. Nauchnyi Mir, Moscow, 351 pp. (in Russian)

Melnikov, V.P., Spesivtsev, V.I., 1995. Engineering-geological and permafrost conditions of the Barents and Kara Shelves. Nauka, Novosibirsk, 198 pp. (in Russian)

Olenchenko, V.V., Shein, A.N., 2013. Possibilities of geophysical methods in the search for Pleistocene megafauna in floodplain and above floodplain deposits of the Yuribei River (Yamal). Kriosfera Zemli XVII (2), 83–92.

Opokina, O.L., Slagoda, E.A., Streletskaya, I.D., Suslova, M.Yu., Tomberg, I.V., Khodzher, T.V., 2010. Cryolithology, hydrochemistry, and microbiology of Holocene limnic and wedge ice in Sibiryakov island of Kara Sea, In: The Origin of Shelf and Archipelagoes in the European Arctic. GEOS, Moscow, pp. 241–247. (in Russian)

Pollard, W., Bell, T., 1998. Massive ice formation in the Eureka Sound Lowlands: A landscape model, in: Permafrost. Proc. of the Seventh Intern. Conf. Québec, Canada, Univ. Laval, Collect. Nordicana 57, pp. 903–908.

Ponomarev, V.M., 1961. Formation of permafrost and groundwater in tidal waters of Arctic seas, in: Physical and Chemical Processes in Freezing and Frozen Rocks. Izd. AN SSSR, Moscow, pp. 95–101. (in Russian)

Robinson, S., Pollard, W., 1998. Massive ground ice within Eureka Sound bedrock, Fosheim Peninsula, Ellesmere Island, N.W.T., in: Permafrost. Proc. of the Seventh Intern. Conf. Québec, Canada, Univ. Laval, Collect. Nordicana 57, pp. 949–954.

Streletskaya, I.D., Leibman, M.O., 2002. Relation of massive ground ice, cryopegs, and their hosts in Central Yamal on the basis of major-ion compositions. Kriosfera Zemli VI (3), 15–24.

Streletskaya, I.D., Vasiliev, A.A., Slagoda, E.A., Opokina, O.L., Oblogov, G.E., 2012. Wedge ice in Sibiryakov Island (Kara Sea). Bull. Moscow University, Ser. 5, Geography 3, 57–63.

Thompson, L.G., Mosley-Thompson, E., Davis, M.E., Bolzan, J.F., Klein, L., Yao, T., Wu, X., Xie, Z., Gundestrup, N., 1989. Holocene – Late Pleistocene climatic ice core records from Qinghai-Tibetan Plateau. Science 246, 474–477.

Usov, V.A., 1967. Cryostratigraphy and formation features of permafrost in a lagoonal coast (a case study of Vilkitsky Island in the Kara Sea). Merzlotnye Issledovaniya 7, 199–210.

Vasil'chuk, A.C., Vasil'chuk, Yu.K., 2010. Local pollen spectra as a new criterion for nonglacial origin of massive ice. Doklady Earth Sci. 433 (1), 985–990.

Vasil'chuk, A.C., Vasil'chuk, Yu.K., 2015. Engineering-geological and geochemical conditions of polygonal landscapes on the Belyy Island (the Kara Sea). Inzhenernaya Geologiya 1, 50–65.

Vasil'chuk, Yu.K., 1992. Oxygen isotope composition of ground ice (application to paleogeocryological reconstructions). Theoretical Problems Department. The Russian Academy of Sciences, Geological Faculty of Moscow University, Research Institute of Engineering Site Investigations. Moscow; vol. 1 – 420 pp., vol. 2 – 264 pp. (in Russian).

Vasil'chuk, Yu.K., 2011. Homogeneous and heterogeneous massive ice in permafrost. Kriosfera Zemli XV (1), 40–51.

Vasil'chuk, Yu.K., 2012. Isotope Methods in the Environment. Part 2: Stable Isotope Geochemistry of Massive Ice. Moscow University Press, Moscow, vol. I, 472 pp. (in Russian)

Vasil'chuk, Yu.K., Budantseva, N.A., Vasil'chuk, A.C., Podborny, Ye.Ye., Sullina, A.N., Chizhova, Ju.N., 2015. Multistage Holocene massive ice near the Sabettayakha River mouth, Yamal Peninsula. Earth's Cryosphere (Kriosfera Zemli) XIX (4), 36–47.

Velikotsky, M.A., 2001. Massive ice in sand bars of the Pechora estuary, in: Solomatin, V.I. (Ed.), Problems of General and Applied Geo-environment of the North, Moscow University Press, Moscow, pp. 148–154. (in Russian)

Wang, B., 1990. Massive ground ice within bedrock. J. Glaciol. Geocryol. 12, 209–218. (in Chinese)

Wang, Sh., Li, W., 1990. First discovery of the deep-buried lake ice in source region of the Yellow River. J. Glaciol. Geocryol. 12, 201–207. (in Chinese)

Received January 12, 2015